Mem. S.A.It. Suppl. Vol. 14, 103

Memorie della
Supplementi

On the Galactic globular cluster ΔV_{HB}^{bump} parameter

A. Di Cecco[1,2], G. Bono[2], A. Pietrinferni[3], R. Becucci[4], P.B. Stetson[6], S. Cassisi[3], S. Degl'Innocenti[4], P. Prada Moroni[4], M. Monelli[5], R. Buonanno[2], C.E. Corsi[1], F. Caputo[1], G. Iannicola[1], I. Ferraro[1], L. Pulone inst 1, and A.R. Walker[7]

[1] Dipartimento di Fisica, Università di Roma Tor Vergata, via della Ricerca Scientifica 1, 00133 Rome, Italy, alessandra.dicecco@roma2.infn.it
[2] INAF–OAR, via Frascati 33, Monte Porzio Catone, Rome, Italy
[3] INAF–OACTe, via Mentore Maggini, 64100, Teramo, Italy
[4] Dipartimento di Fisica, Universitá di Pisa, Largo B. Pontecorvo 3, 56126 Pisa, Italy
[5] IAC – Calle Via Lactea, E38200 La Laguna, Tenerife, Spain
[6] DAO – HIA, 5071 West Saanich Road, Victoria, BC V9E 2E7, Canada
[7] CTIO – NOAO, Casilla 603, La Serena, Chile

Abstract. We calculated new estimates of the ΔV_{HB}^{bump} parameter for 15 Galactic Globular Clusters (GGCs) using accurate ground-based photometric data. We enlarged our sample with literature data and we obtained a sample of 62 GGCs covering a wide metallicity range (-2.16≤[M/H]≤-0.58 dex). To compare the data with the theory we used theoretical models from Pietrinferni et al. (2004, 2006) and two different metallicity scales. We found that the observed values are higher (∼0.4 mag) than the canonical predictions. Moreover, the discepancy increases in the Kraft & Ivans (2003, 2004) metallicity scale and it decreases in the Carretta & Gratton (1997) scale. We investigated also the impact of CNONa extreme mixture and higher He-enhanced abundance (Y = 0.30). The use of these models is not in the direction to explain the observed discrepancy.

Key words. globular cluster: general - stars:horizontal branch - stars: luminosity function

1. Introduction

The Color Magnitude Diagram (CMD) of the GGCs shows an overdensity of star counts in a well determined position along the Red Giant Branch (RGB) phase. The theoretical models indicate that the RGB 'bump' forms when the H-burning shell joins the discontinuity of H abundance left by the previous deep penetration of convective envelope during the 'first dredge-up' (Iben, 1968). The most powerful instrument to detect the bump in observational CMD is the Luminosity Function (LF). In particular, in the cumulative LF the bump appeares as a change in the slope while the differential LF shows an excess of star counts at the bump magnitude. To overcome the uncertainties related to the distance modulus and reddenings we will use the ΔV_{HB}^{bump} parame-

Send offprint requests to: A. Di Cecco

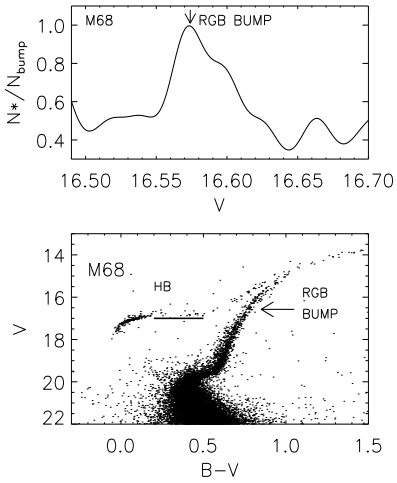

Fig. 1. - Top - RGB LF for the GGC M68. The number of stars (N_*) is normalized to the star number of the bump (N_{bump}). - Bottom - The CMD of M68 in V, B-V bands. The HB level is overplotted and the arrow marks the RGB bump.

ter, which is the difference between the visual bump magnitude and the Horizontal Branch (HB) magnitude at the RR-Lyrae instability strip (Fusi Pecci et al. (1990), hereafter FP90). FP90 found that the predicted bump values were ∼0.4 magnitude brighter than the observed data. Zoccali et al. (1999) found a good agreement between data and predictions using the Carretta & Gratton (1997) (hereafter CG97) scale. In more recent investigation, using new updated models Riello et al. (2003) (hereafter R03) found a good agreement between data and theory for an age of 12±4 Gyr. In the next section we investigate the relation between ΔV_{HB}^{bump} parameter and global metallicity. Moreover, we compare the results with the most recent theoretical predictions.

2. Analysis and results

We calculated the ΔV_{HB}^{bump} for 15 GGCs in the metallicity range $-2.43 \leq [Fe/H] \leq -0.7$ dex. The photometric data were reduced and calibrated using Landolt (1992) standard system. In particular, these data have been taken from Stetson (2000) database. More details concerning the observations can be found at the following URL:http://www4.cadc-ccda.hia-iha.nrc-cnrc.gc.ca/community/STETSON/standards/. To find the RGB bump we generated a gaussian profile with a σ equal to the photometric error for each RGB star detected in V,B-V CMD. Then, we convolved the individual gaussians and we calculated the LF in the RGB region for each cluster. We fitted the bump peak with a gaussian function and we associated to the bump error the gaussian σ. We show the differential LF of M68 ($[Fe/H] = -2.43$ dex) in the upper panel of Fig.1. The HB luminosity level was calculated using the LF in the flat region, which is the region between RR-Lyrae instability strip and the red HB stars. We fitted the LF with a gaussian function and we defined the HB level as the point located at 3 σ fainter than the magnitude of the gaussian peak.

For the GGCs with no red HB, we used a template cluster with the same metallicity and a well populated red HB. To estimate the HB level we shifted the two cluster sequences until they overlapped (Buonanno et al. (1986), Ferraro et al. (1992)). The HB level of M68 is shown in lower panel of Fig.1. The error on ΔV_{HB}^{bump} parameter was estimated by adding in quadrature the bump error and the HB level error obtaining a mean value of ∼0.1 magnitude. To increase the number of the GGCs we extended our sample with the values provided by R03. However, the R03 data were acquired with the F555W band of WFPC2@HST. To transform to the same photometric system we calculated the difference between $\Delta F555W_{HB}^{bump}$ and ΔV_{HB}^{bump} for the seven clusters in common between the two different datasets. On average, the R03 data are 0.06±0.03 higher than our values. The latter quantity was subtracted from the $\Delta F555W_{HB}^{bump}$ values. Owing to the higher statistical detection in the bump region we used our values for the clusters in common. In total, our sample consists of 62 GGCs.

To valuate the effect of the adopted metallicity we decided to use two different metallicity scales, the CG97 scale and the Kraft & Ivans (2003, 2004) (hereinafter KI03,

KI04) scale. The metallicity scale provided by CG97 is based on the homogenization of the iron measurements (FeI and FeII lines) available in the literature, with mean uncertainty on iron abundances ≈0.06 dex. The KI04 metallicity scale is based on the MARCS atmosphere models. The latter metallicity scale has the advantage of using iron measurements based only on FeII lines, that is marginally affected by the non local thermodynamic equilibrium effects (Thevenin & Idiart (1999)). Moreover, this scale is based on robust determinations of surface gravity and effective temperature, and the accuracy is on average better than 0.1 dex. Note that the GC97 measurements are available for the entire cluster sample, whereas the KI04 measurements are given for only 60 clusters. The global metallicity ($[M/H]$) was estimated using the relation provided by Salaris et al. (1993) and assuming an $[\alpha/Fe]$=0.3 dex for all GCs. For the theoretical comparison we used the isochrones and the Zero Age Horizontal Branch (ZAHB) of the BASTI database[1] (Pietrinferni et al. (2004, 2006)). We assumed as canonical values a primordial helium content (Y_p) and an α-enhanced solar chemical mixture. We compared the canonical values with the scaled solar models. The predicted values were calculated assuming an age of 12 Gyr (VandenBerg et al. (2006)) and the theoretical uncertainty is 1.5 Gyr. The comparison between theory and observations as function of global metallicity is shown in Fig.2. As is expected, there is no significant difference (< 0.1 mag) between canonical and solar scaled models when the global metallicity is used. We found that the theoretical predictions understimate the observations independently of the adopted scale. Moreover, we found that the GC97 scale shows a lower discrepancy if compared to the KI04 scale. In the KI04 scale the difference between theory and observations is on average ∼0.4 magnitude and it reaches ∼ 0.6 magnitude in the lower metallicity range ([M/H]≤-2.0 dex). In the CG97 scale the discrepancy with

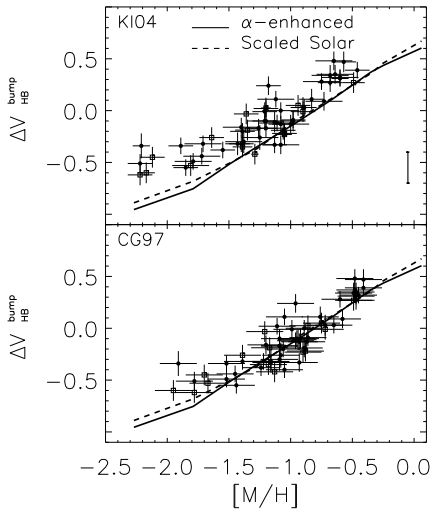

Fig. 2. The ΔV_{HB}^{bump} parameter as function of the KI04 metallicity scale (top) and CG97 scale (bottom). The circles show the data from R03 while the squares mark our data. The solid line shows the predicted values for 12 Gyr. The dashed line shows the scaled solar models. The theoretical uncertainty is plotted as bar in the top right corner.

data is present only in the metal-poor regime ([M/H]≤-1.3 dex). There is much spectroscopic evidence to show that CNO abundance variations exist among stars of the same cluster. Moreover, many other elements like Mg and Al, or O and Na, present anti-correlations.

These features were found not only in the evolved stars but also in unevolved phases and this scenario suggests a self-pollution mechanism internal to the cluster (Ventura & D'Antona (2005)). Bearing in mind these results, we investigated the theoretical ΔV_{HB}^{bump} using the models with CNONa extreme mixture provided by Pietrinferni et al. (2009). The theory developed by Pietrinferni et al. is avaible for structures with metal content $-1.27 \leq [M/H] \leq -0.07$ dex and to investigate the behavior at low metallicity we computed an evolutionary model with [M/H]=-1.81 dex using an updated version of FRANEC (Cariulo et al. (2004),

[1] Evolutionary models can be download at the following URL: http://www.oateramo.inaf.it/BASTI

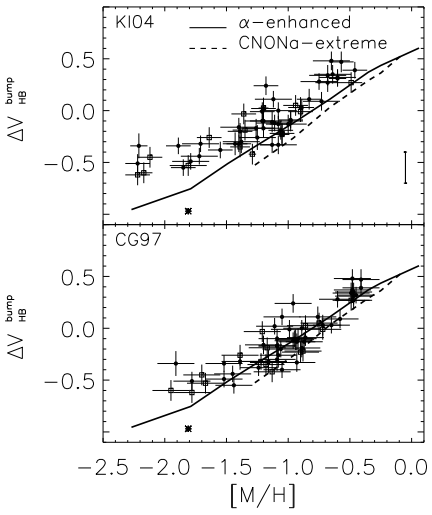

Fig. 3. Same as Fig.2. The solid line shows the canonical values. The dashed line show the CNO-enhanced theory for an age of 12 Gyr and the asterisk marks the 11 Gyr model (see text for more details).

Degl'Innocenti et al. (2008)). This latter model include atomic diffusion which causes a decrease of ∼1 Gyr in the age (Castellani et al. (1997)) and we chose an age of 11 Gyr.

The comparison between CNO-enhanced models and observed data is shown as dashed line in Fig.3 (the asterisk marks the 11 Gyr model). We found that the theoretical ΔV_{HB}^{bump} values are systematially lower than the canonical values and in both scales the CNO-enhanced theory is not able to explain the discrepancy.

Some studies in the last few years showed multiple photometric sequences (Piotto et al. (2007)) that could be interpreted using He-enhanced models. To investigate the impact that a variation of the initial He abundance has on the ΔV_{HB}^{bump} parameter, we used higher He abundance (Y=0.30) models provided by Pietrinferni et al. (2009) The He-enhanced models do not approach to the metal-poor regime ([M/H]≤-1.27 dex) because they do not experience an efficient first dredge-up. We found that the difference with the canonical values is a little bit higher (∼0.1 magnitude) in the metal-rich regime ([M/H]>-0.7 dex) and it is negligible in the metal-intermediate regime (-1.27≤ $[M/H]$ ≤-0.7 dex). This latter effect is due to the fact that both the ZAHB and the RGB bump increase their luminosity. We found that the CNO-enhanced models and the He-enhanced models are not able to explain the discrepancy between theory and observations. Moreover, the discrepancy becomes larger in the metal-poor regime.

References

Buonanno, R., Caloi, V., Castellani, V. et al. 1986, A&AS, 66, 79
Cariulo, P., Degl'Innocenti, S., Castellani, V. 2004, A&A, 421, 1121
Carretta, E., Gratton, R.G. 1997, A&AS, 121, 95 (CG97)
Cassisi, S., Salaris, M., Pietrinferni, A. et al. 2008, ApJ, 672,L115
Castellani, V. et al., 1997, A&A, 322, 801
Degl'Innocenti, S. et al., 2008, Ap&SS, 316, 25
Ferraro, F.R., Clementini, G., Fusi Pecci, F. et al. 1992, MNRAS, 256, 391
Fusi Pecci, F., Ferraro F. R., Crocker, D.A. et al. 1990, A&A, 238, 95 (FP90)
Iben, I. Jr. 1968, ApJ, 154, 581
Kraft, R.P., Ivans, I.I. 2003, PASP, 115, 143
Kraft, R.P., Ivans, I.I. 2004, arXiv:astro-ph/0305380v1
Landolt, A. U., 1992, AJ, 104, 340
Pietrinferni, A., Cassisi, S., Salaris, M., Castelli, F. 2004, ApJ, 612, 168
Pietrinferni, A., Cassisi, S., Salaris, M., Castelli, F. 2006, ApJ, 642, 797
Pietrinferni, A., Cassisi, S., Salaris, M. et al. 2009, ApJ, 697, 275
Piotto, G. et al. 2007, ApJ, 661, L53
Riello, M., Cassisi, S., Piotto et al. 2003, A&A, 410, 553
Salaris, M., Chieffi, A., Straniero, O. 1993, ApJ, 414 580
P. B., Stetson 2000, PASP, 112, 925S
Thevenin, F., Idiart, T. P. 1999, ApJ, 521, 753
VandenBerg, D. A., Bergbusch, P. A., Dowler, P. D. 2006, ApJS, 162, 375
Ventura, P., D'Antona, F. 2005, ApJ, 635, 149
Zoccali, M., Cassisi, S., Piotto, G. et al. 1999, ApJ, 518, 49